

## Investigations on aluminium hybrid composites reinforced with $ZrB_2/Al_2O_3$ /Multi-Walled Carbon Nanotube (MWCNT) for aerospace applications

Elaya Perumal A<sup>a,\*</sup>, Jinu GR<sup>a</sup>, Vidhyalakshmi S<sup>b</sup> and Amal Bosco Jude S<sup>c</sup>

<sup>a</sup>University College of Engineering, Nagercoil, Kanyakumari, Tamilnadu, 629004, India

<sup>b</sup>Nagercoil, Kanyakumari, Tamilnadu, 629004, India

<sup>c</sup>University VOC College of Engineering, Thoothukudi, Tamilnadu, 628008, India

The Aluminium Alloy (AA7050) hybrid composites (AAHC's) reinforced with 2-10 wt.%  $ZrB_2$  ceramic particles, 1-5 wt.%  $Al_2O_3$  particles and 0.5-2.5 wt.% MWCNT in novel Vibro-compo casting through liquid casting route. The  $ZrB_2$  and  $Al_2O_3$  have been introduced in the conventional method, and MWCNT is injected by argon gas. Then, the stirring process was carried out in different temperatures to enhance wettability between reinforcements and matrix. The developed AAHC's were characterised using a Scanning Electron Microscope (SEM) and Energy-dispersive X-ray spectroscopy analysis (EDS). The mechanical properties like hardness, tensile, impact and fatigue tests were performed on all the casted samples elaborately. The dispersion of  $ZrB_2$  ceramic particles and its implanting over the ductile Al7050 matrix was effectively obtained, which shown superior mechanical properties when compared to monolithic Al7050 alloy. The specimen contained 1.5%MWCNT + 6% $ZrB_2$  + 3% $Al_2O_3$  reveals the greater tensile strength, which is 30.73% higher than the base material. Besides, the EDS results ensured the manufacturing of Al 7050/MWCNT +  $ZrB_2$  +  $Al_2O_3$  metal matrix composites successfully, and no other intermetallic phases were identified.

**Keywords:** ceramics, composite materials, metal matrix composites, mechanical properties, metals.

### Introduction

Aluminium alloy hybrid composites are undergoing a revolution in the aerospace industry. The AAHC has received much attention in the past decade. Within the next few years, AAHC, likely to become a significant composite material in aircraft. Currently, aluminium alloy 7050 is used in the wing spar of aircraft structure [1], but it has average strength level. In order to overcome this disadvantage, researchers were focused on this aluminium alloy 7050 to reinforce with TiC [2] and  $TiB_2$  [3].  $Al_3Zr$  dispersoids were reinforced in aluminium alloy 7050 [4]. The  $Al_2O_3$ ,  $ZrB_2$ , SiC, TiC  $TiB_2$  are the most common ceramic materials chosen to reinforce aluminium alloys [5-11]. This paper seeks to address the introduction of multi reinforcements such as MWCNT,  $ZrB_2$ ,  $Al_2O_3$  on aluminium alloy 7050. Several authors have attempted to define AAHC's, but as yet there are still no accepted results on AAHC's. In the literature, there are many composites by aluminium alloy 7050 much work on the potential of AAHC has been carried out. The first studies on AAHC found that aluminium alloy 7050 was reinforced with TiC particles [2]. Experiments on aluminium alloy 7050 reinforced composite were performed by a group of researchers [3].

Lin K [3] has developed and investigated the machinability parameters of  $TiB_2$  particles reinforced with aluminium alloy 7050. They draw focus on monophonic reinforcements such as  $TiB_2$ . It was suggested [12] that, the introduction of  $ZrB_2$  particles on aluminium alloy 6061 has enhanced the properties of composites, and this seems to be a positive approach. Research has tended to focus on the monophonic introduction of reinforcement rather than the multi-entry of reinforcements on aluminium alloy 7050. Baradeswaran [13] contended that aluminium alloy 7075 metal matrix composite enhances the mechanical properties, but they failed to provide adequate information for multi-entry reinforcements. The reinforcements phase have been tried with different weight percentages to improve the mechanical and metallurgical properties of the composite [14-19]. Literature survey reveals that aluminium alloy 7050 rarely reinforced with MWCNT, TiC,  $TiB_2$ ,  $ZrB_2$  and  $Al_2O_3$  in the liquid casting route. Similarly, few research works are identified in hybrid composites using aluminium alloy 7050 as matrix phase. This present work AA7050/MWCNT/  $ZrB_2/Al_2O_3$  hybrid composites were developed through the Vibro compo casting method to get superior interface bonding and increase wettability. Thus, the key objective of this research work is to investigate the influence of the MWCNT,  $ZrB_2$  and  $Al_2O_3$  particles on the mechanical properties such as tensile, microhardness, impact, fatigue and characterised by SEM and EDS on hybrid composites.

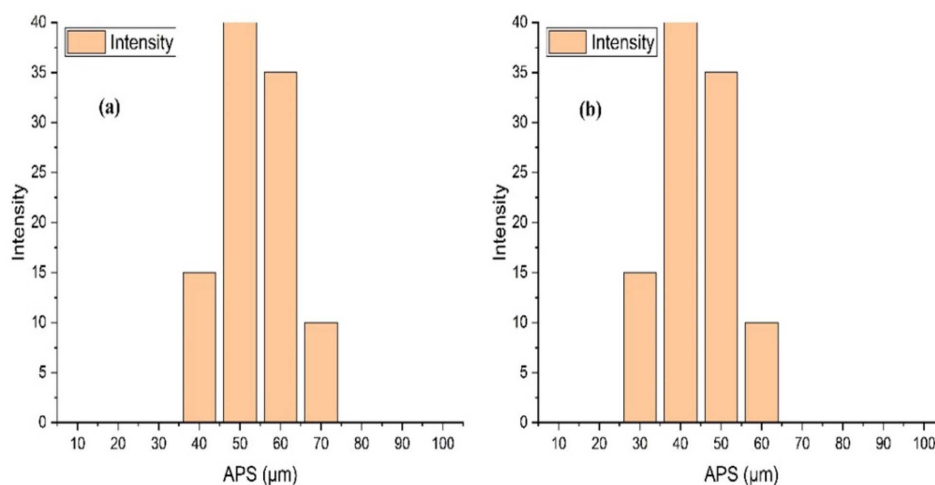
\*Corresponding author:  
Tel : +91-8903966003  
E-mail: skyforplay@gmail.com

**Table 1.** Chemical compositions of Aluminium alloy 7050 [35]

Material	Si	Fe	Cu	Mn	Mg	Ti	Cr	Zn	Zr	Balance
AA7050	0.12 <sub>max</sub>	0.15 <sub>max</sub>	2.0–2.6	0.1 <sub>max</sub>	1.9–2.6	0.10 <sub>max</sub>	0.04 <sub>max</sub>	5.7–6.7	0.08–0.15	Al

**Table 2.** Specifications of  $Al_2O_3$ ,  $ZrB_2$  and Multiwall Carbon Nanotubes

Specifications	$Al_2O_3$	$ZrB_2$	Multiwall Carbon Nanotubes	
			Colour	Black Powder
APS	50-60 $\mu m$	40-50 $\mu m$	Purity	>99%
Form	Powder	Powder	Average Diameter	10-15 nm
Colour	White	Grey/Black	Average Length	~ 5 $\mu m$
Purity	99.9%	99%	Amorphous carbon	<1%
Melting Point	2,072 $^{\circ}C$	3040 $^{\circ}C$	Surface Area	~400 $m^2/g$
Boiling Point	2,977 $^{\circ}C$	-		

**Fig. 1.** (a) Average particle size analysis of  $Al_2O_3$  reinforcement, (b) Average particle size analysis of  $ZrB_2$  reinforcement.

## Materials and Methods

### Materials

In an attempt to do AAHC, Aluminium Alloy 7050-T7451 chosen as matrix phase and its chemical composition given in Table 1. The Multiwall Carbon Nanotubes (MWCNT),  $ZrB_2$  and  $Al_2O_3$  were chosen for the reinforcement phase and their specifications mentioned in Table 2. The MWCNT supplied by AdNano Technologies, Catalytic carbon vapour deposition (CCVD) process were used to produce ultrapure multiwall Carbon Nanotubes. The received  $Al_2O_3$ ,  $ZrB_2$  particles have been examined to confirm the size of the particles using Average particle size analyser. The average particle size of  $Al_2O_3$  is 50  $\mu m$  and  $ZrB_2$  is 40  $\mu m$  is confirmed, as shown in Fig. 1(a) and 1(b). Similarly, the received MWCNT's are analysed by scanning electron microscopy equipment in the 100 nm  $\times$  60,000 and 100 nm  $\times$  30,000 scale. The SEM results confirm the presence of MWCNT's, as shown in Fig. 2(a) and 2(b). Transmission Electron Microscopic analysis results are shown in Fig. 2(c). The Raman spectroscopy examination was conducted on MWCNT's, and its results show good agreement with wavenumber and

Raman intensity in Fig. 2(d). The percentage of weight loss examination of the MWCNT was performed against temperature; weight loss percentage is nearly to zero at 700  $^{\circ}C$  in Fig. 2(e). XRD analysis was done on MWCNT, and the result exhibits the chemical composition peaks of MWCNT's are shown in Fig. 2(f).

### Fabrication method

The fabrication of composites carried out through liquid metallurgy route via Vibro compo casting method. In this work, a specific vibrator is attached with a crucible for superior dispersion of MWCNT in the aluminium matrix. This method is in line with a substantially the same as that used by Abbasipour [20] compo casting setup with some modifications. The apparatus is consisting of alumina crucible with muffle furnace, coated steel stirrer, reinforcement injection tube, crucible with a vibrator is attached with the compo casting equipment, which is shown in Fig. 2(g). The melt temperature has measured by using the K-type thermocouple, and Argon gas is used to inject the reinforcements to the vortex melt. The compo casting equipment can easily be customised to suit all the conditions. It was decided that the best equipment for

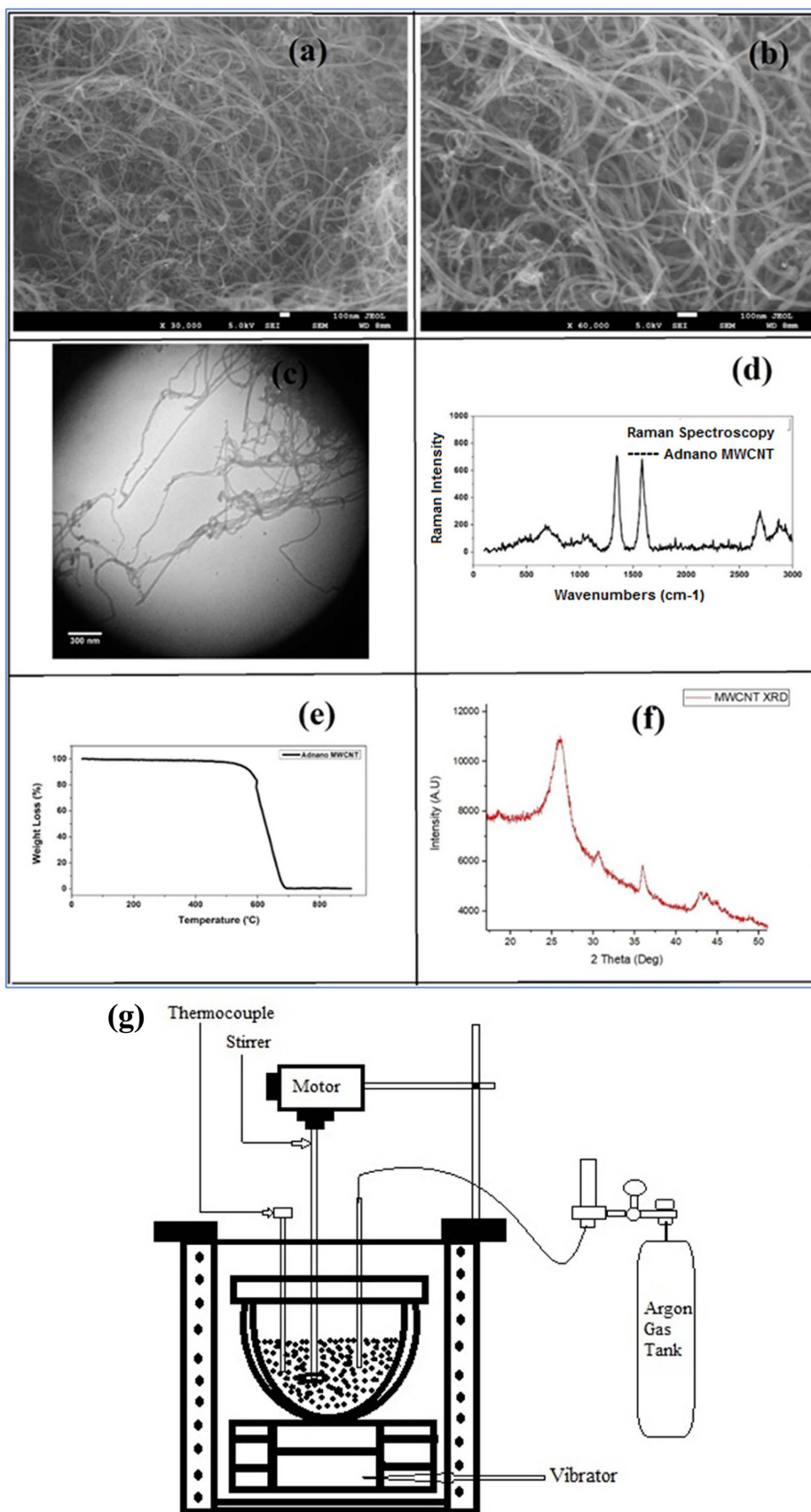


**Fig. 2.** (a), (b) and (c), Scanning Electron Microscopic and Transmission Electron Microscopic images of MWCNT's, (d) Raman spectroscopy analysis of MWCNT, (e) Weight loss analysis of MWCNT against temperature, (f) XRD analysis of MWCNT's, (g) Schematic Diagram of Stir casting setup.

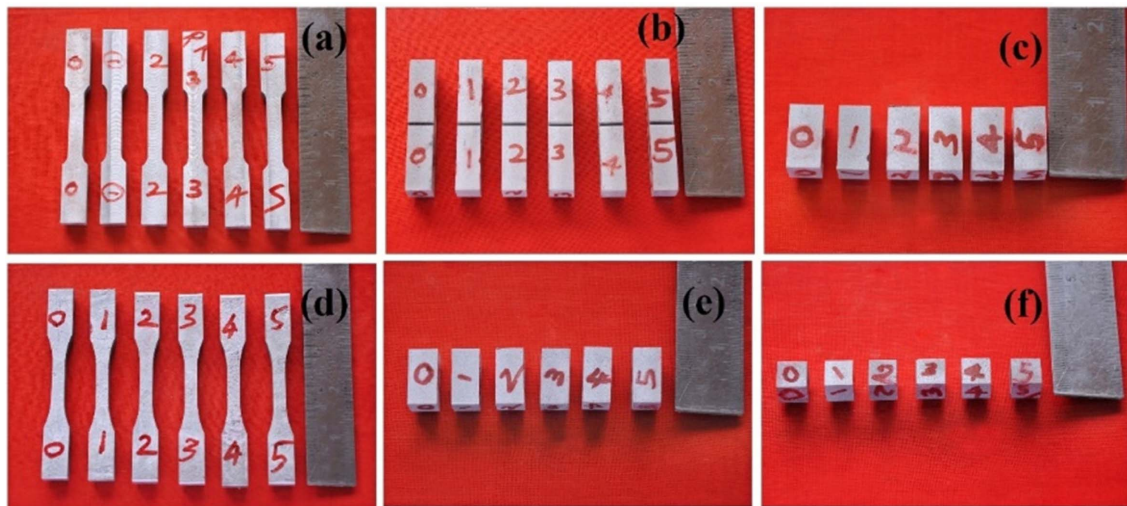


**Fig. 3.** Machined samples for Tensile, Impact, Micro Hardness, Fatigue, SEM and EDAX Investigations.

this investigation because it is one of the most suitable methods for casting Carbon Nanotubes. All samples have prepared in the following two routes. Initially,  $ZrB_2$  and  $Al_2O_3$  introduced in the traditional route, and MWCNT's are injected and stirred in different temperatures to enhance wettability between reinforcements and matrix. Crucible was allowed to vibrate and preheated at 600 °C then aluminium alloy 7050 is melted at 700 °C. The Preheated  $ZrB_2$  and  $Al_2O_3$  were mixed with aluminium melt then stirred at speed 450RPM. MWCNT were injected by argon gas to the semi-solid aluminium melt then stirred at 250RPM to enhance good wettability of MWCNT's. Finally, the molten metal has poured in  $100 \times 100 \times 10$  mm sized dye. Then, the samples were machined as per various ASTM standards by ELECTRA wire EDM machine (SPRINTCUT WIN-Pulse Generator: ELPULS 40A DLX. Fig. 3(a)-3(f) show the machined samples for various mechanical and tribological investigations.

### Characterisation

The Tensile strength analysis has carried out on the  $100 \times 6 \times 12$  mm sized samples shown in Fig. 3(a) as per ASTM standard E8M04 by Computerised Universal Testing Machine TMC– CUTM – 50 kN model, Chennai. Then, Microhardness examinations were Examined on the  $20 \times 10 \times 6$  mm sized samples shown in Fig. 3(c) as per ASTM standard E18M by using Microhardness Testing Machine, Mitutoyo– HM113 Model, Japan. Izod impact tests have performed on  $75 \times 10 \times 10$  mm sized samples shown in Fig. 3(b) as per ASTM standard D256 using Impact testing machine. Fatigue strength investigation was conducted using computerised fatigue equipment supplied by AVJ Engineering Services Coimbatore. Similarly, material characterisations such as Scanning Electron Microscope – SEM, JEOL– JSM 6390, Japan and Energy Dispersive Spectroscopy – EDS, Oxford Instruments– INCA Energy 250 LN2

Closed, UK was used and conducted.

## Results and Discussion

### Mechanical properties of AA7050/MWCNT/ $ZrB_2/Al_2O_3$ AAHC'S

#### Tensile test

The internal resistive force against the load of the composites was enhanced due to superior dispersion in matrix till the AA7050/ (1.5%MWCNT + 6%  $ZrB_2$  + 3% $Al_2O_3$ ) composite, as shown in Fig. 4(a). From the Fig. 4(b), the ultimate tensile strength of B, C and D composites are in increase trend while other two in downfall. The ultimate tensile strength of E and F composites are decreasing due to the increment of MWCNT,  $ZrB_2$  and  $Al_2O_3$  particles and porosity due to the new cluster formation. The  $ZrB_2$  particles are surrounded by MWCNT's. There is no Interfacial bonding due to the lack of aluminium matrix phase in those composites. It is due to the non-uniform dispersion between matrix and reinforcements.

#### Micro hardness test

The Vickers microhardness values of all casted samples are examined. The Vickers Hardness Number is directly proportional to the reinforcement's weight percentage. An increasing trend was observed on AA7050/(0.5%MWCNT + 2%  $ZrB_2$  + 1% $Al_2O_3$ ), AA7050/(1%MWCNT + 4% $ZrB_2$  + 2% $Al_2O_3$ ), AA7050/(1.5%MWCNT + 6% $ZrB_2$  + 3%  $Al_2O_3$ ), AA7050/(2%MWCNT + 8%  $ZrB_2$  + 4%  $Al_2O_3$ ) and AA7050/(2.5%MWCNT + 10%  $ZrB_2$  + 5%  $Al_2O_3$ ) composites as shown in Fig. 4(c), which reveals the increase of  $ZrB_2$ ,  $Al_2O_3$  and MWCNT reinforced with aluminium matrix enhance the Vickers hardness value.  $Al_2O_3$  ceramic particle was obstacles for the dislocation movement [21-23]. The  $Al_2O_3$  particles protect the aluminium alloy 7050 from infiltration and cutting of slides on the surface of the composites [24, 25].

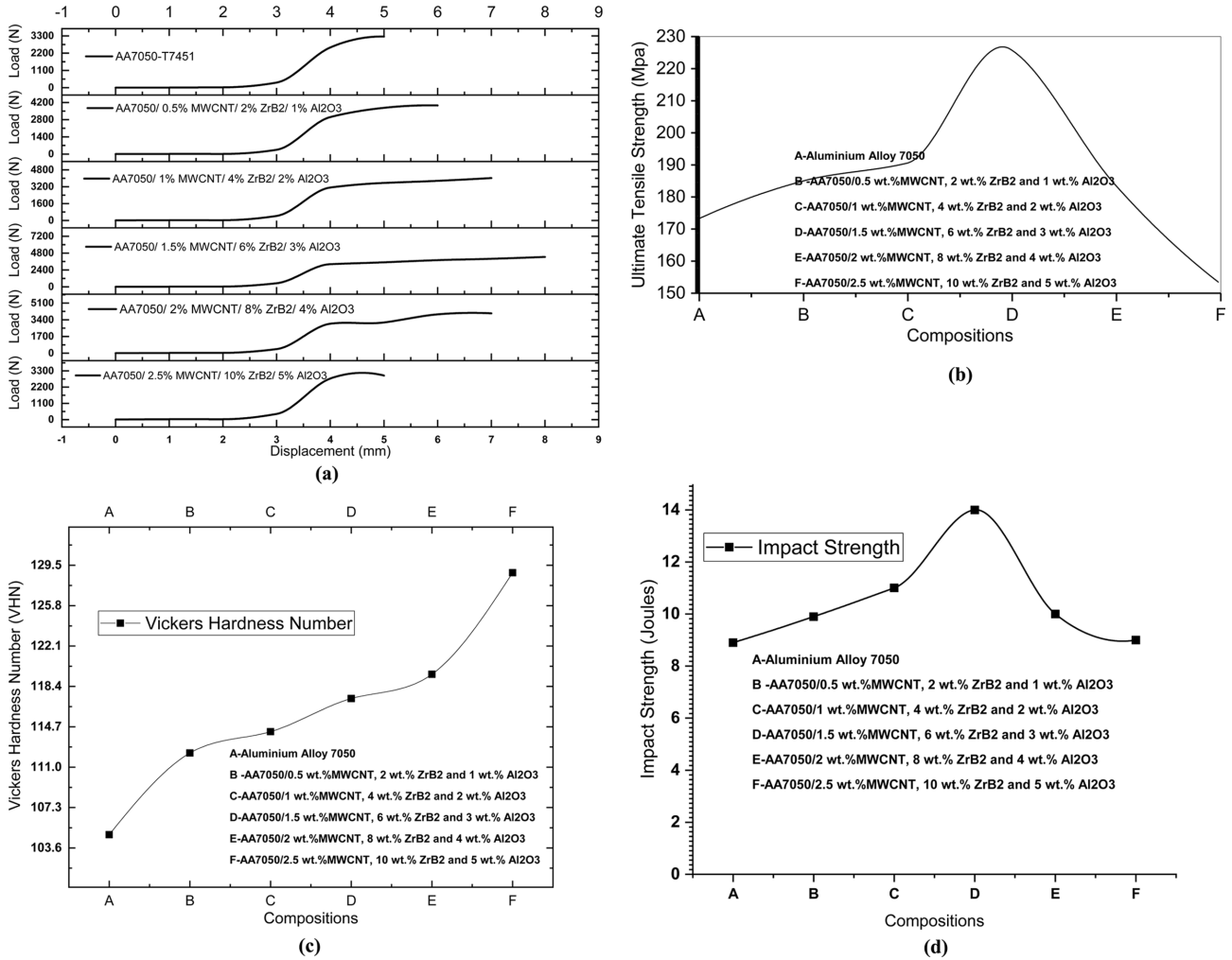


**Fig. 4.** (a) Load versus displacement curve for the tensile test of Hybrid composites, (b) Ultimate tensile strength of Hybrid composites, (c) Vickers Hardness Number of Hybrid composites, (d) Impact Strength of Hybrid composites.

**Impact test**

Impact test results reveal the increasing trend in impact strength till the AA7050/(1.5%MWCNT + 6% Zr<sub>2</sub>B<sub>3</sub> + 3%Al<sub>2</sub>O<sub>3</sub>) composite, as shown in Fig. 4(d). Then, downfall trend is observed in AA7050/(2% MWCNT + 8%Zr<sub>2</sub>B<sub>3</sub> + 4%Al<sub>2</sub>O<sub>3</sub>), and AA7050/(2.5% MWCNT + 10%Zr<sub>2</sub>B<sub>3</sub> + 5%Al<sub>2</sub>O<sub>3</sub>) composites due to its fragile nature because of more percentage of reinforcements in the aluminium matrix. The AA7050/(0.5% MWCNT + 2%Zr<sub>2</sub>B<sub>3</sub> + 1%Al<sub>2</sub>O<sub>3</sub>), AA7050/(1%MWCNT + 4%Zr<sub>2</sub>B<sub>3</sub> + 2%Al<sub>2</sub>O<sub>3</sub>) and AA7050/(1.5%MWCNT/6% Zr<sub>2</sub>B<sub>3</sub>/3%Al<sub>2</sub>O<sub>3</sub>) composites ensure the proper wettability and superior dispersion of reinforcements in the aluminium alloy 7050 matrix.

**Fatigue test**

The fatigue strength was examined on all casted composites as results shown in Fig. 5(a) to 5(f). The hybrid composite revealed the fatigue resistance concerning load and time mentioned in Table 3. Fig. 5(a) shows the casted aluminium alloy AA7050 has an average fatigue strength. The increasing fatigue strength identified

in Fig. 5(b) to 5(d). The AA7050 specimen has fatigue strength up to 200N load at 10<sup>6</sup> cycles then failures at 10<sup>1</sup> cycles when the load increased to 220N. Similarly, the fatigue strength and failure limit for all casted composites were mentioned in Table 3. The composite AA7050/(1.5%MWCNT + 6%Zr<sub>2</sub>B<sub>3</sub> + 3%Al<sub>2</sub>O<sub>3</sub>) has enhanced fatigue strength to withstand the cyclic stresses. These cyclic stresses lead to fatigue cracking, which is below the static yield strength of the hybrid composite. The Fig. 5(e) and 5(f) show the fatigue strength was significantly reduced in E and F hybrid composites due to the existence of higher reinforcement percentage, which leads to brittle phenomenon [26-30].

**Microstructure of MWCNT/ Zr<sub>2</sub>B<sub>3</sub>/ Al<sub>2</sub>O<sub>3</sub> AAHC'S**

The SEM images of casted MWCNT/ Zr<sub>2</sub>B<sub>3</sub>/ Al<sub>2</sub>O<sub>3</sub> AAHC'S is depicted in Fig. 6(a) - 6(f). Fig. 6(a) indicates the SEM image of the casted Aluminium Alloy 7050. The SEM microstructure image of hybrid composite AA7050/(0.5%MWCNT + 2% Zr<sub>2</sub>B<sub>3</sub> + 1%Al<sub>2</sub>O<sub>3</sub>) is shown in Fig. 6(b), which reveals the porosity and shrinkages presence are less, which ensures the quality of Vibro

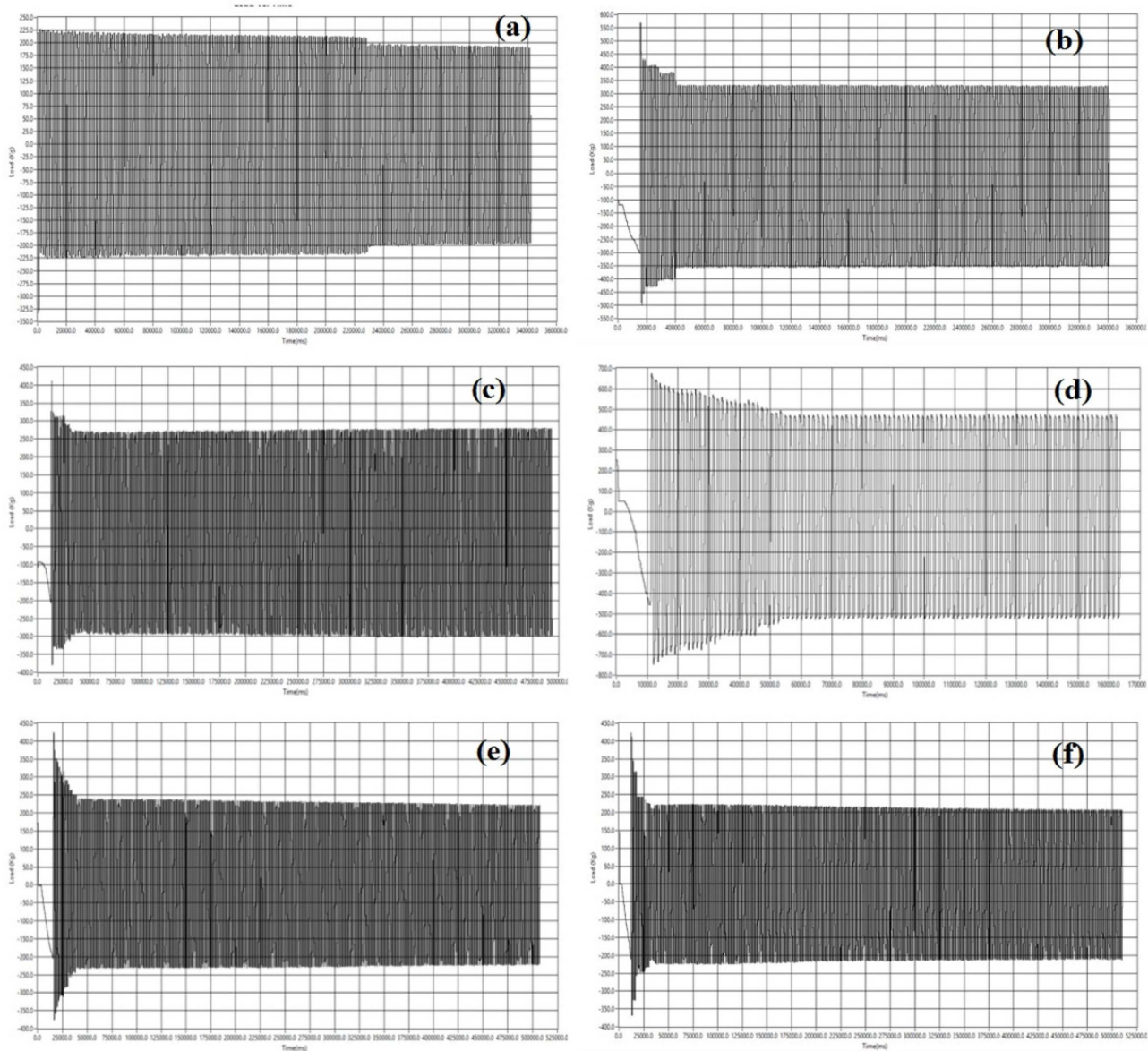


**Fig. 5.** Results of fatigue cycles for time and Load; (a) AA7050, (b) AA7050/(0.5%MWCNT + 2% $ZrB_2$  + 1% $Al_2O_3$ ), (c) AA7050/(1%MWCNT + 4% $ZrB_2$  + 2% $Al_2O_3$ ), (d) AA7050/(1.5%MWCNT + 6% $ZrB_2$  + 3% $Al_2O_3$ ), (e) AA7050/(2%MWCNT + 8% $ZrB_2$  + 4% $Al_2O_3$ ), (f) AA7050/(2.5%MWCNT + 10% $ZrB_2$  + 5% $Al_2O_3$ ).

compo casting and the similar trend was absorbed in the AA7050/(1%MWCNT + 4%  $ZrB_2$  + 2% $Al_2O_3$ ) hybrid composite shown in Fig. 6(c). The SEM microstructure image of AA7050/(1.5%MWCNT + 6% $ZrB_2$  + 3% $Al_2O_3$ ) exposes the dendritic structure of matrix alloy has disappeared due to the presence of the MWCNT,  $ZrB_2$ , and  $Al_2O_3$  reinforcements as shown in Fig. 6(d). The SEM microstructure images of AA7050/(2%MWCNT + 8% $ZrB_2$  + 4% $Al_2O_3$ ) and AA7050/(2.5%MWCNT + 10% $ZrB_2$  + 5% $Al_2O_3$ ) are shown in Fig. 6(e) and Fig. 6(f). This reinforcement particles influence the grain formation in the semi-solid state of composite material and enhance the better solidification. More grain refinement has been achieved by finer grains due to reinforcements. The intragranular distributions have found

on casted samples, which enhances the mechanical and tribological properties. The influencing parameters for the distribution of reinforcements are convection current, buoyant motion and movement of particles [31]. The solidification front's velocity has a significant role in deciding intra or intergranular distribution. It has formed when the velocity of the solidification front is above the critical velocity, which is between  $10^{-3}$  to  $10^{-5}$  m/s [32]. The temperature gradient is the influencing factor for the critical velocity and particle size. The SEM images are showing the clear interface between the aluminium matrix and the following reinforcements MWCNT,  $ZrB_2$ , and  $Al_2O_3$ . Moreover, no reaction products and interfacial reactions are identified between the reinforcements. Various researchers reported that

**Table 3.** Fatigue Load obtained, cycles completed and result in the condition of Hybrid composites

Hybrid Composite Specimen	Load obtained in the graph (N)	Result condition	Cycles completed
AA7050	114	No Failure	$10^6$
	200		
	220	Failure	$10^1$
AA7050/ (0.5%MWCNT + 2% $ZrB_2$ + 1% $Al_2O_3$ )	114	No Failure	$10^6$
	180		
	260		
	300	Failure	$10^1$
AA7050/ (1%MWCNT + 4% $ZrB_2$ + 2% $Al_2O_3$ )	110	No Failure	$10^6$
	154		
	206		
	270	Failure	$10^1$
300			
AA7050/ (1.5%MWCNT + 6% $ZrB_2$ + 3% $Al_2O_3$ )	120	No Failure	$10^6$
	154		
	240		
	285		
	330		
	366		
	415		
	460		
	500		
AA7050/ (2%MWCNT + 8% $ZrB_2$ + 4% $Al_2O_3$ )	120	No Failure	$10^6$
	169		
	230	Failure	$10^1$
250			
AA7050/ (2.5%MWCNT + 10% $ZrB_2$ + 5% $Al_2O_3$ )	115	No Failure	$10^6$
	156		
	210	Failure	$10^1$
250			

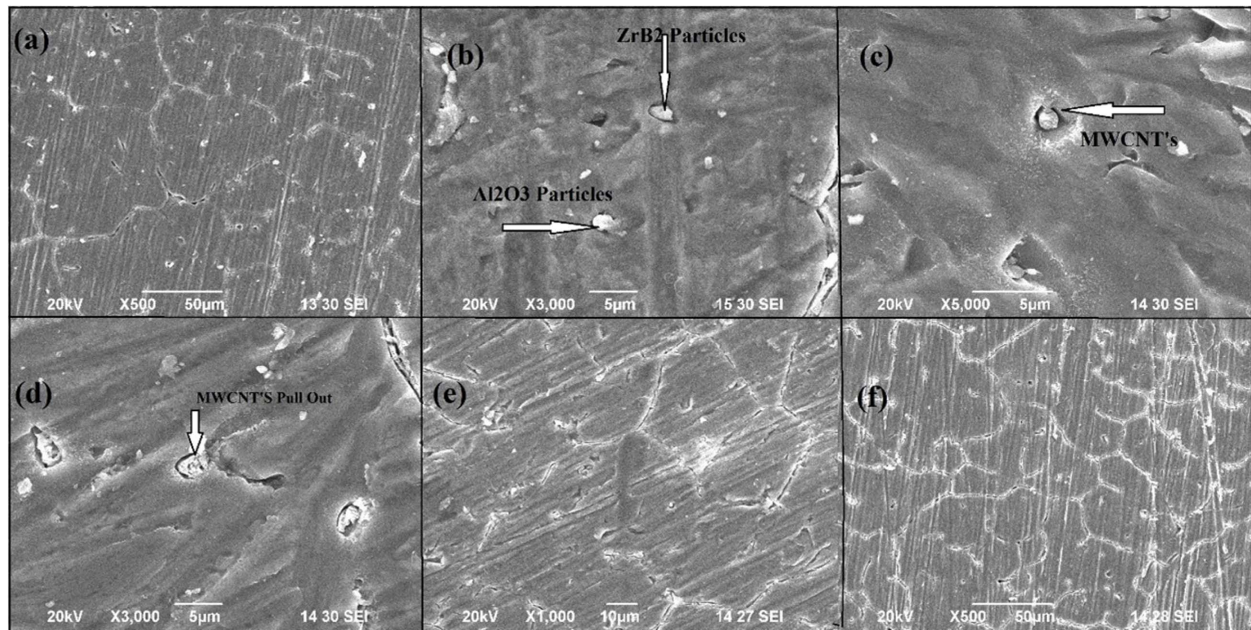


**Fig. 6.** (a) SEM microstructure images of AA7050, (b) SEM microstructure images of AA7050/(0.5%MWCNT + 2% $ZrB_2$  + 1% $Al_2O_3$ ), (c) SEM microstructure images of AA7050/(1%MWCNT+4% $ZrB_2$  + 2% $Al_2O_3$ ), (d) SEM microstructure images of AA7050/(1.5%MWCNT + 6% $ZrB_2$  + 3% $Al_2O_3$ ), (e) SEM microstructure images of AA7050/(2%MWCNT + 8% $ZrB_2$  + 4% $Al_2O_3$ ), (f) SEM microstructure images of AA7050/(2.5%MWCNT + 10% $ZrB_2$  + 5% $Al_2O_3$ ).

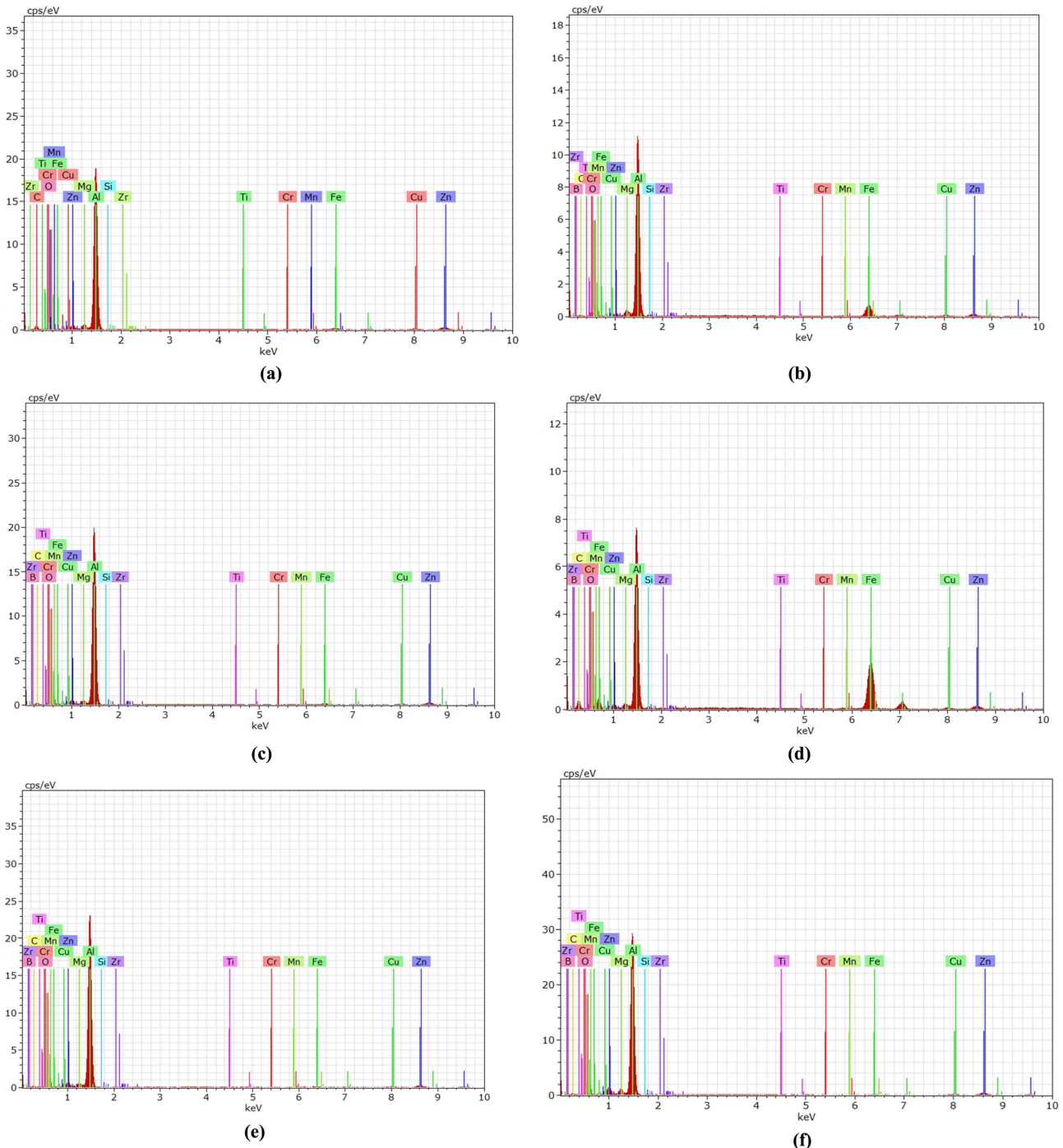


**Fig. 7.** (a) EDS test analysis of AA7050, (b) EDS test analysis of AA7050/(0.5%MWCNT + 2% $Zr_2B_2$  + 1% $Al_2O_3$ ), (c) EDS test analysis of AA7050/(1%MWCNT + 4% $Zr_2B_2$  + 2% $Al_2O_3$ ), (d) EDS test analysis of AA7050/(1.5%MWCNT + 6% $Zr_2B_2$  + 3% $Al_2O_3$ ), (e) EDS test analysis of AA7050/(2%MWCNT + 8% $Zr_2B_2$  + 4% $Al_2O_3$ ), (f) EDS test analysis of AA7050/(2.5%MWCNT + 10% $Zr_2B_2$  + 5% $Al_2O_3$ ).

the reaction products would surround the particle and weaken the interfacial strength when a reaction occurs [33-36].

#### EDAX Results of MWCNT/ $Zr_2B_2$ / $Al_2O_3$ AAHC'S

Fig. 7(a) shows the Energy Dispersive Spectrum of cast Aluminium Alloy 7050 and with its elements. The high-intensity peak elements are representing Aluminium, zinc, copper and magnesium, and low-intensity peak

elements for ferrous, Silicon, Manganese, Titanium, Chromium and Zirconium are identified. The Fig. 7(b) shows EDS analysis of hybrid composite AA7050/(0.5%MWCNT + 2% $Zr_2B_2$  + 1% $Al_2O_3$ ) with Carbon, Zirconium diboride and alumina. Similarly, no other elements present in the AA7050/(1%MWCNT + 4% $Zr_2B_2$  + 2% $Al_2O_3$ ) hybrid composites as Fig. 7(c) and hybrid composite AA7050/(1.5%MWCNT + 6% $Zr_2B_2$  + 3% $Al_2O_3$ ) as Fig. 7(d). The presence of elements of

AA7050-MWCNT/ZrB<sub>2</sub>/Al<sub>2</sub>O<sub>3</sub> is rich in the casted samples AA7050/(2%MWCNT + 8%ZrB<sub>2</sub> + 4%Al<sub>2</sub>O<sub>3</sub>) and AA7050/(2.5%MWCNT + 10%ZrB<sub>2</sub> + 5%Al<sub>2</sub>O<sub>3</sub>) as shown in Fig. 7(e) and 7(f). The EDS result reveals that no elemental presence due to its interfacial reaction between the matrix and reinforcements.

### Conclusion

The Mechanical characteristics and microstructure study of Vibro-compo cast AA7050 + MWCNT + ZrB<sub>2</sub> + Al<sub>2</sub>O<sub>3</sub> aluminium hybrid composites were studied in detail. The following achieved conclusions are drawn:

The superior interface bonding and wettability between the reinforcement and AA 7050 matrix were achieved by novel Vibro compo casting method. The ultimate tensile strength is enhanced by about 30.73% in Hybrid composite compared with the base material. The impact strength and microhardness of AA7050 hybrid composite reveal the increasing trend. The tension-tension fatigue strength of hybrid composites confirms the superior fatigue strength against the applied cyclic loadings. The SEM images show the uniform dispersion between the matrix and MWCNT, ZrB<sub>2</sub> and Al<sub>2</sub>O<sub>3</sub> reinforcements. EDS results reveal all elements of both matrix and reinforcements are present in casted hybrid composite materials.

### Conflict of Interest

There is no conflict of interest.

### Acknowledgement

Corresponding author (A. ELAYA PERUMAL) gratefully acknowledges the financial support from the Ministry of Social Justice & Empowerment and Ministry of Tribal Affairs, Government of India. This research work was supported by the Ministry of Social Justice & Empowerment and Ministry of Tribal Affairs, Government of India, under RGNF Scheme [Award Number: F117.1/201617/RGNF201517SCTAM 25495]

### References

1. P. Rambabu, N.E. Prasad, V.V. Kutumbarao, and R.J.H. Wanhill, in "Aerospace Materials and Material Technologies" (Springer Singapore, 2017) p.29-52.
2. A. Ranganathan, P.V. Akshay Krishnan, A.S. Nambiar, S. Mohan Kumar, and V. Ravi Kumar, *Mater. Today Proc.* 5[11] (2018) 25368-25375.
3. K. Lin, W. Wang, R. Jiang, and Y. Xiong, *Int. J. Adv. Manuf. Technol.* 100[1-4] (2019) 143-151.
4. J.D. Robson and P.B. Prangnell, *Acta Mater.* 49[4] (2001) 599-613.
5. J.J. Zhuang, X.Y. Zhang, B. Sun, R.G. Song, and H. Li, *Gongcheng Kexue Xuebao/Chinese J. Eng.* 39[10] (2017) 1532-1539.
6. V. Mohanavel, S. Suresh Kumar, T. Sathish, and K.T. Anand, in: *Mater. Today Proc.* 5[5] (2018) 13601-13605.
7. M.T. Sijo and K.R. Jayadevan, *Procedia Technol.* 24 (2016) 379-385.
8. K. Ravi Kumar, K. Kiran, and V.S. Sreebalaji, *J. Alloys Compd.* 723 (2017) 795-801.
9. A. Chandana, I.D. Lawrence, and S. Jayabal, in: *Mater. Today Proc.* 5[6] (2018) 14317-14326.
10. S. Poria, P. Sahoo, and G. Sutradhar, *Silicon* 8[4] (2016) 591-599.
11. M. Narimani, B. Lotfi, and Z. Sadeghian, *Surf. Coatings Technol.* 285 (2016) 1-10.
12. S.R. Ruban, K.L.D. Wins, M.M. Boopathi, and A.A. Richard, *Int. J. Mech. Eng. Technol.* 9[2] (2018) 88-94.
13. A. Prakash, M. Dharmendra Kumar, A. Baradeswaran, R. Padma Priya, and A. Bagubali, *J. Balk. Tribol. Assoc.* 24[1] (2018) 1-14.
14. N. Panwar and A. Chauhan, in: *Mater. Today Proc.* 5[2] (2018) 5933-5939.
15. R. Sharma, S.J. P. K. Kakkar, K. Kamboj, and P. Sharma, *Int. Res. J. Eng. Technol.* 4[2] (2017) 832-842.
16. N. Gangil, A.N. Siddiquee, and S. Maheshwari, *J. Alloys Compd.* 715 (2017) 91-104.
17. S.T. Mavhangu, E.T. Akinlabi, M.A. Onitiri, and F.M. Varachia, *Procedia Manuf.* 7 (2017) 178-182.
18. C.T. Lynch and J.P. Kershaw, in "Metal Matrix Composites" (CRC, 2018) p.1-170.
19. Yashpal, Sumankant, C.S. Jawalkar, A.S. Verma, and N.M. Suri, in: *Mater. Today Proc.* 4[2] (2017) 2927-2936.
20. B. Abbasipour, B. Niroumand, and S.M. Monir Vaghefi, *Trans. Nonferrous Met. Soc.* 20[9] (2010) 1561-1566.
21. K. Shirvanimoghaddam, S.U. Hamim, M. Karbalaie Akbari, S.M. Fakhrohoseini, H. Khayyam, A.H. Pakseresht, E. Ghasali, M. Zabet, K.S. Munir, S. Jia, J.P. Davim, and M. Naebe, *Compos. Part A Appl. Sci. Manuf.* 92 (2017) 70-96.
22. Ş. Karabulut, U. Gökmen, H. Çinici, *Compos. Part B Eng.* 93 (2016) 43-55.
23. S. Sahraeinejad, H. Izadi, M. Haghshenas, A.P. Gerlich, *Mater. Sci. Eng. A* 626 (2015) 505-513.
24. V. Mohanavel, K. Rajan, P. V. Senthil, and S. Arul, in: *Mater. Today Proc.* 4[2] (2017), 3093-3101.
25. B.C. Kandpal, J. Kumar, and H. Singh, in: *Mater. Today Proc.* 4[2] (2017) 2783-2792.
26. R. Narayanan, C. Saravanan, V. Krishnan, and K. Subramanian, *Mech. Mech. Eng.* 19[1] (2015) 23-30.
27. D. Patidar and R.S. Rana, in: *Mater. Today Proc.* 4[2] (2017) 2981-2988.
28. M. Shukla, S.K. Dhakad, P. Agarwal, and M.K. Pradhan, in: *Mater. Today Proc.* 5[2] (2018) 5830-5836.
29. G. Moona, R.S. Walia, V. Rastogi, and R. Sharma, *Indian J. Pure Appl. Phys.* 56[1] (2018) 164-175.
30. V.C. Kale, *IOSR J. Mech. Civ. Eng.* 12[6] (2015) 31-36.
31. R. Bauri, D. Yadav, and G. Suhas, *Mater. Sci. Eng. A* 528[13-14] (2011) 4732-4739.
32. G. Wilde, M. Byrnes, J.H. Perepezko, *J. Non. Cryst. Solids* 250-252 (1999) 626-631.
33. P.S. Bains, S.S. Sidhu, and H.S. Payal, *Mater. Manuf. Process.* 31[5] (2016) 553-573.
34. A. V. Muley, S. Aravindan, and I.P. Singh, *Manuf. Rev.* 2[15] (2015) 1-13.
35. M.O. Bodunrin, K.K. Alaneme, and L.H. Chown, *J. Mater. Res. Technol.* 4[4] (2015) 434-445.
36. M. Kannaiyan, J.G. Raghuvaran, K. Govindan, and E.P. Annamalai, *J. Ceram. Process. Res.* 21[1] (2020) 26-34.